This is the resubmitted (not the final printed) version of the manuscript. For referencing please refer to the final article found at doi:
10.1016/j.quascirev.2013.07.015

Changes in current patterns in the Fram Strait at the Pliocene/Pleistocene boundary

Gebhardt, A. C., Geissler, W. H., Matthiessen, J., and Jokat, W.

Alfred Wegener Institute Helmholtz Centre for Polar and Marine Research, Am Alten Hafen 26, 27568 Bremerhaven, Germany

1 Abstract

Seismic reflection profiles from the northwestern and central part of the Fram Strait show thick packages of drift type sediments mainly along the western Yermak Plateau flank, but also in the central, flat part of the Fram Strait. North of 80.5°N, a large-scale field of sediment waves along the Yermak Plateau rise separates a western, lower from an eastern, upper drift body. These drift bodies were deposited by bottom currents, most likely the northbound Yermak Branch of the West Spitsbergen Current, but we cannot rule out that the western drift body may also have been influenced by southbound bottom currents. A stratigraphic boundary is clearly visible within the drift bodies and even more pronounced within the sediment waves, separating a lower package of waves migrating upslope at low angle (~5°) from an upper package with significantly increased wave crest migration (~16.5°). This stratigraphic boundary could be tracked along the seismic network and corresponds to the lithostratigraphic boundary between units IA and IB at ODP Leg 151, Site 911 that was dated to 2.7 Ma. The increase in wave-crest migration angle indicates a shift towards higher sedimentation rates at 2.7 Ma, which corresponds to the intensification of the Northern Hemisphere glaciation with a major expansion of the Greenland, Scandinavian, northern Barents Sea and North American ice sheets. The subaerially exposed Barents shelf and the expansion of the northern Barents Sea ice sheet (as well as Svalbard) are likely sources for enhanced erosion and enhanced fluvial input along the pathway of the West Spitsbergen Current, resulting in higher sedimentation rates in the Fram Strait.

Keywords: drift sediments; contourite; seismic reflection; Pliocene/Pleistocene; Fram Strait; Yermak Plateau; Arctic Ocean

2 Introduction

The Fram Strait is the only deep-water connection between the North Atlantic and the Arctic Ocean, and this narrow gateway channels both inflowing relatively warm and saline North Atlantic as well as outflowing cold and less saline water. Sediments along the eastern flank as well as in the central part of the Fram Strait are deposited mainly as contourites influenced by these currents (e.g., Eiken and Hinz, 1993; Howe et al., 2008). The Arctic Ocean and its surroundings are highly sensitive to climate change, and paleoclimate reconstructions in the Arctic realm have thus become a major research focus during the past decade (e.g., Jakobsson et al., 2010; Melles et al., 2012; Moran et al., 2006; Tripati et al., 2008). Paleoclimate change in the Arctic Ocean led to significant shifts in the current patterns (e.g., Haley et al., 2008; Knies et al., 2007), and since almost all Arctic water masses traverse the Fram Strait upon leaving the Arctic Ocean, it is highly likely that the changes in the current patterns would somehow be recorded in the Fram Strait sediments. Studying these sediments therefore helps to unravel the paleocurrent patterns in the Arctic Ocean and, thus, get a better insight into paleoclimate change that affected the Arctic realm.

In this study, we use a network of seismic reflection data (i) to map the sediment structures and geometries along the western flank of the Yermak Plateau and in the central part of the Fram Strait, and (ii) to identify changes in the sedimentation regime.

3 Study area

The area investigated in this current study comprises the Fram Strait and the adjacent western flank of the Yermak Plateau (Fig. 1). The Fram Strait is the only present deep-water connection between the North Atlantic and Arctic Ocean (Eiken and Hinz, 1993). It is located between the Svalbard Archipelago to the East and Greenland to the West between 78°N and 82°N and has a water depth of up to 3,000 m and a width of 200 km. The bow-shaped Yermak Plateau is located north of the Svalbard archipelago with water depths of 700 to 800 m over large parts. The initial basement topography of the Yermak Plateau is rather rough with many deep troughs separating the basement heights (Geissler et al., 2011; Jokat et al., 2008). Cenozoic sediments of up to 4 km in thickness almost level this initial topography (Geissler et al., 2011) with exceptions of some basement heights such as the Sverdrup Bank that is still outcropping and not yet leveled completely. The sediments are generally well-layered and can mostly be interpreted as contourite deposits along the basement heights, deposited by bottom currents. Large parts of the Yermak Plateau exhibit glacial overprint of

the uppermost sediment layers indicated both by an overconsolidated diamicton and by mega-scale lineations of deep-keeled tabular icebergs and curvilinear plow marks of smaller, single icebergs (e.g., Dowdeswell et al., 2010; Gebhardt et al., 2011; Jakobsson et al., 2010; O'Regan et al., 2010; Vogt et al., 1994), but the western flank is characterized by well-layered drift-type sediments (e.g., Gebhardt et al., 2011; Geissler et al., 2011; Pulm, 2010).

3.1 Evolution of the Fram Strait

Even though seafloor spreading in the central Atlantic propagated northwards as early as in the late Cretaceous, the Arctic Ocean stayed isolated from the Atlantic Ocean probably until the separation of the Yermak Plateau from northeast Greenland some 35 Ma ago (Ehlers and Jokat, 2013; Jokat et al., 2008; Moran et al., 2006). The onset of significant water exchange through the Fram Strait, however, is still under debate, but deep water exchange and, thus, ventilation of the Arctic Ocean, is likely to have started at 18.2 Ma, and a significant deepening of the Fram Strait is documented from 17.5 Myrs on (Jakobsson et al., 2007). The abyssal plain in the northern Fram Strait is underlain by young oceanic crust and the Lena Trough is still active as the current spreading center (Läderach et al., 2011).

3.2 Oceanographic circulation through the Fram Strait

The Fram Strait is channeling the flow of surface and deep waters between the Arctic and North Atlantic and allows the deep-water exchange between both polar hydrospheres (Fig 1). The currents flowing from the North Atlantic through the Norwegian Sea and towards the Arctic Ocean include the northward inflow of relatively warm and saline waters via the Norwegian Current and further as the West Spitsbergen Current along the western margin of Svalbard, and the southward outflow of cold and low saline waters along the Greenland shelf via the East Greenland Current (e.g., Bourke et al., 1988; Manley et al., 1992; Rudels et al., 2012) (Fig. 1). Within the Fram Strait, the West Spitsbergen Current splits into three components north of approximately 78°N (e.g., Quadfasel et al., 1987; Rudels et al., 2002). One component, the Spitsbergen Branch, turns eastward directly north of the Svalbard archipelago and flows along the shallow southern Yermak Plateau (Schauer et al., 2004). The second branch, the Return Atlantic Current, re-circulates towards south between 78° and 80°N (Bourke et al., 1988), and the third branch, the Yermak Branch, transports water northwards along the western Yermak Plateau and enters the Arctic Ocean through the eastern Fram Strait, turning eastward at the northeastern tip of the plateau (Rudels et al., 2002) (Fig. 1). Within the Arctic Ocean, the warm water mass mixes with cold and fresh surface waters, and sea ice formation during Arctic winters enhances its salinity and, thus, its density. The water mass sinks, and flows as an intermediate water mass counterclockwise

before being exported out of the Arctic Ocean via the Fram Strait along the east Greenland shelf as part of the East Greenland Current (Rudels et al., 2012).

3.3 Age information

All age information used for this study is derived from ODP Leg 151, Sites 909 and 911 (Fig. 2). The northern profiles (shown: AWI-20040040, 20040080, 20040150, 20040160; Figs. 3-6) were dated following the stratigraphic correlations of Geissler and Jokat (2004) and Geissler et al. (2011). These authors used information from correlations of seismic lines with ODP Site 911, Leg 151. Site 911 was drilled in triplicate in summer 1993 (Myhre et al., 1995) with RV *Joides Resolution* with 911A at 80°28.466'N, 8°13.640'E being the deepest hole (terminal depth 505.8 mbsf). Hole 911A was drilled in 901.6 m water depth at the eastern flank of the Yermak Plateau (Fig. 1). The sediment record of Site 911 was described as homogeneous silty clay and clayey silt, and was divided into lithological subunits IA and IB (Myhre et al., 1995) at 380.4 mbsf with the upper unit containing significantly more dropstones than the lower one. The boundary between the two subunits was dated to ~2.7 to 2.8 Ma (Myhre et al., 1995; Sato and Kameo, 1996) and corresponds to the base of seismostratigraphic unit YP-3 (Eiken and Hinz, 1993; Geissler and Jokat, 2004).

Age information for the southwestern profiles (shown: AWI-97253; Fig. 6) derives from correlations of seismic lines with ODP Site 909, Leg 151. Site 909 was drilled in triplicate in summer 1993 with *RV Joides Resolution* with Hole 909C at 78° 35.096' N, 3° 4.222' E being the deepest hole (terminal depth 1061.80 mbsf). Hole 909C was drilled in 2518 m water depth immediately north of the Hovgård Ridge (Fig. 1) (Myhre et al., 1995). The sediment record from Site 909 was subdivided into 3 lithological units I, II and III with the lowermost subdivided into subunits IIIA and IIIB. Unit I spans the sediments between 0 and 248.8 mbsf and is dated to Quaternary to middle Pliocene (0 to ~3.6 Ma; Winkler et al., 2002). It consists of interbedded clay, silty clay and clayey mud and contains dropstones of >1 cm in size (Myhre et al., 1995). Unit II consists of more massive silty clay interbedded with thinner layers of carbonate-rich clays without dropstones and contains the sediments between 248.8 and 518.3 mbsf dated to Pliocene to Miocene age (~3.6 to 6-7 Ma; Winkler et al., 2002) age. Unit III contains the sediments below 518.3 mbsf (Myhre et al., 1995). Unit III can be further subdivided into IIIA and IIIB at 923.4 mbsf which corresponds to middle Miocene age (Winkler et al., 2002). Subunit IIIA consists of silty and clayey sediments with meter-scale intervals of thin bioturbated layers and laminations (Myhre et al., 1995). The sediments of Subunit IIIB are folded and deformed and have a basal age of Early to Middle Miocene (Winkler et al., 2002).

In order to correlate the southern to the northern profiles, we additionally used information from Knies et al. (2009) who place the magnetostratigraphic Matuyama-Gauss boundary

(2.581 Ma) at 186.40 mbsf for Hole 909C. This boundary is very close to the YP-3/YP-2 boundary that was used in the northern profiles; at Hole 911A, these two boundaries are only some 20 m apart (360 mbsf for the 2.581 Ma Matuyama-Gauss boundary vs. 380.4 mbsf for the 2.7-2.8 Ma YP-3/YP-2 boundary).

4 Data acquisition and processing

Hydroacoustic and seismic data along the western flank of the Yermak Plateau were collected mostly in parallel during *RV Polarstern* expedition ARK-XVIII/2 (Jokat, 2003) in 2002 and ARK-XX/3 in 2004 (Stein, 2005), and profiles from the central part of the Fram Strait were collected during *RV Polarstern* expedition ARK-XIII/3 (Krause, 1998) in 1997 and, again, ARK-XVIII/2 in 2002. Navigation and positioning of all profiles used GPS in connection with the ship's integrated inertial navigation system (MINS). Sediment echosounder data were acquired with the hull-mounted PARASOUND system (Atlas Hydrographic, Germany; P70) installed on *RV Polarstern*. Bathymetric data were collected with the *RV Polarstern's* deep-water multibeam system DS-2 (Atlas Hydrographic, Germany) that operates on a frequency of 15.5 kHz. A transmission beam aperture of 90° was used during both expeditions, resulting in a swath width of twice the mean water depth. Bathymetric data were processed thoroughly comprising outlier rejection and editing of the navigation data using CARIS-HIPS (Jokat, 2003; Stein, 2005). Sediment echosounder and bathymetric data were used for comparison with the seismic reflection profiles for better understanding of the sediment geometries and their according deposition and transport mechanisms. Seismic data were processed using standard techniques (CMP sorting, NMO corrections, f-k filtering, stacking, and bandpass filtering) (Geissler et al., 2011). Tracklines of all profiles used in this study are shown in Fig. 1.

5 Description of seismic profiles

Throughout our investigation area, the entire western flank of the Yermak Plateau is characterized by large-scale sediment bodies. The lowest part of the sediment packages (YP-1; Figs. 3 to 5) fills and levels the troughs of the rather rough acoustic basement (see also Geissler et al., 2011). The upper two seismostratigraphic units (YP-2 and YP-3) exhibit well-layered internal geometries that are quite similar over large N-S distances. The geometries do not alter significantly from the lowermost to the uppermost part of each individual unit, and layers are slightly thinner towards east and west and thicker in their middle part where they bend (best visible in Fig. 4). The stacked layers build up a long, elongated mound body relative to the lower boundary of the according seismostratigraphic

units, and the crests of the layers migrate towards east. The line that connects the crests has a slightly sigmoidal curve. Such sediments are commonly interpreted as contourite or drift sediments (e.g., Faugères et al., 1999). In the case of the Yermak Plateau, these contourite sediments occur in a scale of thousands of square kilometers. Also the central part of the Yermak Plateau is leveled by thick packages of contourite sediments that fill the deep valleys and troughs of the rough acoustic basement topography (Geissler et al., 2011), but the uppermost part is eroded and incised by a grounded ice sheet and by keels of deep-draft mega-scale tabular icebergs (e.g. Dowdeswell et al., 2010; Gebhardt et al., 2011). Turbidite fans also build up large sediment bodies with well-layered internal geometries, but turbidites are often transported through turbidite channels before they are deposited. Such channels were not encountered at the western flank of the Yermak Plateau during the 2002 and 2004 expeditions. Furthermore, turbidite deposits would be expected at the deeper water depths, and not at the upper flank of the Yermak Plateau. The sediment facies encountered at the Yermak Plateau flank continues onto the top of the plateau. Also, turbidites would likely be thickest at their proximal and thin out towards their distal end, which is in contradiction with the geometries found in the sediment packages at the western Yermak Plateau flank. And furthermore, even though both turbiditic levées as well as contourite drifts tend to migrate downsteam, this would be in a downslope direction for the turbiditic depositions (Faugères et al., 1999), while at the Yermak Plateau, the crests move slightly upwards the slope. In conclusion, the sediments encountered here can definitely be interpreted as drift or contourite bodies rather than turbidite fans. It is however possible that further downstream of the current, e.g. at the Svalbard continental slope, turbidites bring sediment particles in suspension that are later deposited along the Yermak Plateau flanks.

North of 80.5°N, two drift bodies were encountered along the western flank of the Yermak Plateau. The two drift bodies are separated by a field of sediment waves. The western, lower drift body, hereafter referred to as drift body A, is located at water depths of 2500 to 3500 m, the eastern, upper drift body, named drift body B, comprises the flank at water depths <1630 m. In the more central, deeper part of the Fram Strait, contourite sediments were observed in several seismic profiles and can be interpreted as drift body A. In the following, a detailed description of selected seismic profiles is given. All tracklines of these profiles are shown in Fig. 1.

Profile AWI-20040040 was shot from the Lena Trough in the west to the Sverdrup Bank on the central flat part of the Yermak Plateau (Fig. 1), with the western Yermak Plateau flank between CDPs 3200 and 7200 (Fig. 3). The acoustic basement exhibits a rough topography and is overlain by thick packages of rather well-layered sediments west of CDP 6200, while the same packages are much thinner in the central Fram Strait area. At CDP 7200, a topographic height of the basement was encountered, and sediment cover is thin or absent

west of this topographic height. Seismostratigraphic units YP-3 and YP-2 exist both on the Yermak Plateau and in the evolving Fram Strait area and extending towards the Lena Trough, while the oldest unit YP-1 was likely only deposited on the Yermak Plateau. Some faults are imaged at CDPs 4000, 5150, and 6600. A large slump scar marks the transition of the rather smooth, flat upper part to a more inclined, steeper, lower part of the flank between CDPs 5200 and 5700. Here, thick packages of YP-3 are missing. Both seismostratigraphic units YP-3 and YP-2 can be interpreted as drift bodies deposited by contourite currents along the western flank of the Yermak Plateau. Roughly between CDPs 5800 to 6100, sediment waves could be detected both in YP-3 and YP-2, separating the more western drift body A from eastern drift body B. The area in which sediment waves could establish in older unit YP-2 is slightly more towards east than in younger unit YP-3.

Profile AWI-20040150 is much shorter than AWI-20040040 and only spans the western flank of the Yermak Plateau. Seismostratigraphic units YP-3 and YP-2 are well-stratified and exhibit the two drift bodies A and B separated by two packages of sediment waves of different age between CDPs 1300 and 1800 (Fig. 4), very similar to what is observed in AWI-20040040. In AWI-20040150, however, the lower sediment wave package is much less pronounced than the upper one. YP-1 underlies YP-2 but its internal structures are less well imaged.

Profile AWI-20040160 spans from the Lena Trough across the entire central Yermak Plateau. The acoustic basement shows a rough topography overlain by thick packages of YP-1 sediments (Fig. 5). These seem to extend into the Lena Trough, but are much thinner there than below the Yermak Plateau flank. YP-1 does not show much internal details of sedimentary structures, but the overlaying YP-2 and YP-3 again exhibit the two drift bodies A and B separated by a distinct field of sediment waves between CDPs 1200 and 1800 (Fig. 6). Between CDPs 600 and 800, a very local field of smaller-scale sediment waves is observed, likely associated with a relative basement height at this position.

Profile AWI-97253 is located more towards south, in the central part of the Fram Strait, and spans from the Greenland shelf in the west to the northernmost end of the Molloy Deep in the east (Fig. 7). This profile exhibits a drift body in its western part between CDPs 2100 and 3800, and a channel-levée complex between CDPs 3800 and 5100 (Berger, 2009). Lithostratigraphic units I, II and III defined at ODP Leg 151 Site 909 were correlated through the seismic network and are indicated in this profile; unit I is subdivided into IA* and IB* with IA* comprising the uppermost 2.581 Ma according to a chronology by Knies et al. (2009) for site 909. All units are characterized by well-layered sediments with drift-type characteristics; stratigraphic boundaries are non-erosive and concordant.

6 Interpretation and discussion

The western drift body A is clearly separated from the eastern drift body B north of 80.5°N (Pulm, 2010). It is located along the lowest western Yermak Plateau rise and extends towards the central Fram Strait north of 80.5°N, and covers almost the complete central Fram Strait south of 80.5°N (Fig. 8). Sediment layers are concave in YP-2 and fill the troughs of the rough acoustic basement. At the YP-3/YP-2 boundary, they are almost leveled, and they are flat to slightly concave slope-upwards in YP-3 (Figs. 3, 5). The layers do not show a significant decrease in thickness from the central region towards its margins except very local examples such as the trough fill shown in fig. 3 (CDPs 6700 to 7200). Within YP-2, all sediment layers are thinner on the western and thicker on the eastern, slopeward side. Using the theory that coriolis force-related deposition occurs to the right side of the flow direction on the northern hemisphere (Faugères and Mulder, 2011; Faugères et al., 1999), this suggests a formation by a northbound bottom current whose center is located where the thin layers are encountered. This is most pronounced on profile AWI-20040040 (Fig. 3). Also profile AWI-20040160 (Fig. 5) suggests a northbound current that formed drift body A at least in its lower part. For YP-3, however, the flow direction of the associated current cannot reliably be determined from the sediments; a modeling study by Schlichtholz and Houssais (1999) suggests southbound deep water currents at depths larger than 1500 m. This would imply that drift body A was likely formed by a northbound current in unit YP-2 and by a southbound current in unit YP-3. Smaller-scale sediment waves found between CDPs 600 to 800 in AWI-20040160 overlay a relative basement height that is not yet completely leveled and may act as a local obstacle in the otherwise smooth present topography, and as such induce the formation of these smaller-scale sediment waves.

A second, significantly larger field of sediment waves is observed in all profiles along the western slope of the Yermak Plateau, separating drift bodies A and B (Figs. 3-6, 8). The sediment-wave field is formed in water depths of ~2500 to 1600 m. Sediment waves are often associated with drift bodies and occur where slopes change their angle significantly, as is the case for the observed area.

Crests of sediment waves normally are oriented perpendicular to the current by which they are formed. Sediment waves consisting of fine-grained material, however, tend to be oriented more obliquely to the current (Howe et al., 1998), and sediment waves on slopes (slope angle >2° at the wave field location; Pulm, 2010) typically have low angles of ~10° to 50° to the flow (Wynn and Masson, 2008). Fig. 9a shows that the crests of the sediment waves move upslope, which suggests that they were generated by a current with a slight upslope component. It is however unclear if this is the current associated with drift body A or B, respectively. Figure 9b shows the crests of some of the sediment waves. They are oriented roughly in N-S direction, but with a slight angle towards NNW-SSE in the more southern and

towards NNE-SSW in the more northern part. One sediment wave obviously has a curvilinear crest shape, but the swath of the bathymetry data is too small to resolve the crest geometry reliably. The general alignment of the sediment waves points at a north- or southbound bottom current but does not allow specifying more precisely. The angle between the more southern and the more northern crests points at a slight rotation of the bottom current in this area.

The sediment waves are generally well-layered with wavelengths of 1500 to 2000 m and amplitudes in the range of 3 to 10 m (Fig. 9a). The entire package of sediment waves can be subdivided at the boundary between seismostratigraphic units YP-2 and YP-3 where a significant change in the outer shape of the waves is observed. Here, the angle in which the wave crests migrate upslope changes from ~5° in the older YP-2 waves to much steeper ~16.5° in the younger YP-3 waves (Pulm, 2010). The YP-2 sediment waves show sedimentation only on the upslope side of the wave, while the downslope side is characterized by non-deposition or even erosion (Fig. 9a). The younger sediment waves of YP-3, in contrast, show net deposition on both the upslope and the downslope side (Pulm, 2010). This points at a significant change in bottom current speed and/or sediment supply from lower sedimentation rates and stronger currents in older YP-2 to enhanced sedimentation rates along with lower current speeds in the younger YP-3 (Wynn and Masson, 2008).

Eastern drift body B is located on the continental slope at water depths <1630 m and is visible in the seismic data throughout the entire western Yermak Plateau slope, and it extends onto the central part of the Yermak Plateau (Gebhardt et al., 2011; Geissler et al., 2011) (Fig. 8). The crest of drift body B is gradually migrating upslope within YP-3 as well as within YP2, but at the boundary between the two units, shape and location of the crest change significantly and abruptly from a more western position in YP-2 to a more eastern position in YP-3. The stratigraphic boundary between YP-3 and YP-2 is non-erosive and concordant along the flanks throughout the entire investigation area. Using the classification of Faugères and Stow (2008), drift body B can be interpreted as a mounded drift, likely of "plastered drift" type accumulated by a fairly constant, low-velocity current. This can be stated for both the younger YP-3 and the older YP-2 part of the drift body; internal sediment structures within YP-1 are not imaged clearly enough to interpret its accumulation mechanism reliably.

Drift body B lies in the flow path of the Yermak Branch of the West Spitsbergen Current. This northbound current transports heat from the North Atlantic into the Arctic Ocean. Furthermore, this current is characterized by a high suspension load in the bottom layer, which is also mirrored in a rich benthic fauna along its track (Rutgers van der Loeff et al., 2002). It is quite likely that this current deposited large parts of the thick sediment packages

that fill and almost level the rough basement topography of the Yermak Plateau as described for example in Geissler et al. (2011). The change in sedimentation that is visible at the YP-2/YP-3 boundary does not affect the general shape of the drift body but rather its relative position on the western Yermak Plateau flank, i.e. the drift body is moved upslope. This suggests that not only the upper part of this drift body, but also the older YP-2 part was likely deposited associated with a northbound bottom current. Only locally and associated with topographic heights, the bottom currents on the central Yermak Plateau may be deflected and flow in opposite direction (Gebhardt et al., 2011).

In spring 2002, an oceanographic profile was measured along approximately 81.33°N on the Swedish icebreaker *IB Oden* (Rudels et al., 2005). The easternmost station of this profile was located at ~82°N just west of the Yermak Plateau, somewhat north of profile AWI-20040040. The Yermak Branch was only identified east of the zero meridian in this oceanographic profile, while southbound flow was measured west of it. This would mean that drift body A could be influenced also by a southbound current in its westernmost part; topography however is complicated in this area and deflection of both the northbound and the southbound currents are highly likely. Drift body A, in our opinion, does not show significant signs of a southbound current in nearby profile AWI-20040040, but we can also not exclude that at least temporarily a southbound current may influence this drift body.

Further to the south, in profile AWI-97253, a channel-levée complex is visible (Fig. 7). While the northeastern flank of the Fram Strait, i.e. the Yermak Plateau flank, is mainly influenced by lateral sediment transport processes (Howe et al., 2008; Pulm, 2010), downslope processes are common on the entire Greenland side (Berger and Jokat, 2008, 2009; Ó Cofaigh et al., 2004). The study by Ó Cofaigh et al. (2004) revealed the northeast Greenland continental margin as an area with an extensive system of submarine channels with turbidites formed predominantly during full glacial and deglacial conditions. A study by Eiken and Hinz (1993) on several seismic profiles from along the entire western Spitsbergen slope showed the occurrence of mixed turbidite/contourite deposits also on the eastern Fram Strait flank south of ~80°N. The drift body that was described west of the channel-levée complex can therefore be interpreted in this context as deriving from a mixed turbidite/contourite system. The influence of downslope sediment processes from the Greenland shelf is also obvious from an erosive, large-scale mass movement deposit, likely a debris flow, that is intercalated in the well-layered sediments of the drift body with an age somewhat younger than the IA*/IB* boundary, i.e. younger than 2.6 Ma. The channel-levée complex identified on profile AWI-97253 likely is not a typical turbidite channel as it has overbank deposits on both sides, but formed due to the highly variable topography around the Molloy Deep in combination with the local bottom currents. Within the channel-levée complex, both a northbound current in the eastern and a southbound current in the western part can be

derived from the large step-like levees confining the entire channel (Fig. 7), following the general theory that contourite behaviour and coriolis force-related deposition is to the right of the flow direction (e.g., Faugères and Mulder, 2011). During the past two decades, several oceanographic profiles were measured along ~79°N, i.e. south of profile AWI-97253 (e.g. Beszczynska-Möller et al., 2012; Schauer et al., 2004). These profiles show that the Atlantic Return Current is turning exactly in this area around the Molloy and Hayes Deeps, which is in good agreement with our data.

The large-scale drift bodies deposited in the entire eastern Fram Strait are associated with the northbound West Spitsbergen Current in the southern part, and from the Yermak Branch and the Spitsbergen Branch in which the West Spitsbergen Current is split north of the Svalbard Archipelago. Since not only the southernmost Yermak Plateau and the western flank are characterized by large drift bodies, but in fact the entire central part of the rough basement topography of the plateau is filled in and leveled by thick packages of such sediments, it is likely that the bottom current pattern is much more complicated in this area, with a bottom current flowing like a large sheet over the entire range in between the Yermak and the Spitsbergen Branch. This is confirmed by a modeling study by Schlichtholz and Houssais (1999). This large current system is locally disturbed by obstacles such as relative basement heights (e.g. around the Sverdrup Bank; Gebhardt et al., 2011), but the general flow trend is SW-NE. Along the western Yermak Plateau flank, the Yermak Branch flows northwards and turns towards northeast only at about 81.5°N, following the topography of the plateau. At around 82°N, the plateau exhibits a roughly SE-NW trending bedrock sill that functions as a large obstacle and likely reduces the current speed. Current velocities decrease significantly along the pathway of the northbound currents in the Fram Strait: Fahrbach et al. (2001) report velocities of up to 24 cm s^{-1} in the near bottom layer of the core of the West Spitsbergen Current at 79°N, and (Schlichtholz and Houssais, 1999) modeled velocities as low as 1 to 3 cm s^{-1} for the Yermak Branch (named Yermak Slope Current in their study). A gradient within the current speeds with a decreasing trend towards north could also be responsible for a discrepancy in the sediment patterns encountered between the southern and northern part of the Fram Strait. Signs of erosion were found in the southern part, at the Vestnesa drift (Howe et al., 2008), i.e. where current velocities are high. Towards north, the drift bodies show parallel layering, and further north divergent layering becomes more and more dominant (Pulm, 2010). Water masses carry a high suspension load along the northwestern Svalbard continental slope, and this sediment load is deposited where current velocities are lower, resulting in parallel layering within the drift bodies. Towards north, divergent layering witnesses the decrease in sedimentation (Pulm, 2010).

The most striking feature in the entire sediment succession along the western Yermak Plateau flank is the distinct change in sediment geometries at the YP-3/YP-2 boundary, i.e.

401 at ~2.7 Ma. This change is best visible in the sediment waves and less distinct in the drift
402 bodies (Figs. 3-5, 9). This change is synchronous with the onset of the Northern Hemisphere
403 glaciation that is commonly assumed for ~2.7 Ma (e.g., Haug et al., 2005). Prior to 2.7 Ma,
404 the Arctic realm was mostly ice-free, and temperatures were significantly higher than today
405 (Brigham-Grette et al., 2013; Ravelo, 2010). A gradual or stepwise cooling since
406 approximately 3.6 Ma was described by many authors (e.g.,Brigham-Grette et al., 2013;
407 Flesche Kleiven et al., 2002; Mudelsee and Raymo, 2005). But even though the initiation of
408 large-scale glaciation of the northern hemisphere started already approximately 1 million
409 years earlier, ice-sheet development in Greenland, Scandinavia and North America was
410 initiated approximately synchronously at 2.72-2.73 Ma (Flesche Kleiven et al., 2002)., and
411 also in northwestern Svalbard, glaciers reached the shelf break at around 2.6 to 2.8 Ma
412 (Sarkar et al., 2011). It seems that also the current system in the Fram Strait has changed
413 significantly at the same time. This change apparently did not happen gradually, and it is
414 quite likely that it is closely related to the development of the ice sheets in the Fram Strait
415 hinterland mainly in the Barents Sea and Svalbard area. In profile AWI-97253 from the
416 southern Fram Strait, the YP-3/YP-2 boundary could not be spotted (seismostratigraphic
417 correlation with the Yermak Plateau ODP sites 910-912 impossible), but instead the 2.6 Ma
418 timeline defined at ODP site 909 (Knies et al., 2009) is indicated (IA*/IB* boundary, Fig. 6).
419 Here, this timeline does not coincide with a change in the sediment pattern, so the change
420 did possibly only affect the northern Fram Strait, not the southwestern part. The change in
421 sediment wave geometries and migration angle indicate a significant increase of
422 sedimentation rates at ~2.7 Ma. Such an increase could be reached by an enhanced
423 suspension load of the water masses that are depositing drift body B and the sediment
424 waves. The respective currents flow along the Norwegian and the Svalbard continental
425 margin and incorporate fluvial and fluvioglacial input, and the proximity of glaciers at the
426 northwestern Svalbard shelf break (Sarkar et al., 2011) could have served as a source for
427 suspended material. Enhanced erosion on both Scandinavia and the Svalbard Archipelago
428 would enrich the suspension load of the West Spitsbergen Current. Butt et al. (2002, and
429 references therein) showed in a modeling study comprising the past 2.3 Ma that the Barents
430 shelf was subaerially exposed at 2.3 Ma, and only at around ~1.0 Ma major parts of the shelf
431 became marine. Laberg et al. (2010) showed that in the Barents Sea region, glaciers
432 terminated on land in the Barents Sea region between 2.7 and 1.5 Ma, and sediment was
433 transported to the paleo-shoreline in a glaciofluvial manner. After 1.5 Ma, glaciers reached
434 the shelf break and sediment transport occurred subglacially (Laberg et al., 2010), and Knies
435 et al. (2009) show a large-scale intensification of glaciation in the Barents Sea at around 1
436 Ma. This region, therefore, likely acted as a major source for additional suspension load of
437 the West Spitsbergen Current. Enhanced suspension load of the currents could also be

achieved by higher velocities along the Norwegian and Svalbard margin, resulting in higher energies and, thus, higher erosion rates. The currents slow down towards north, and sedimentation of the suspended material can take place. An exposed Barents shelf would not only lead to higher subaerial erosion rates, but also hinder the inflow of Atlantic waters north of Scandinavia through the Barents Sea and the St Anna Trough into the Arctic Ocean, as is currently the case (Butt et al., 2002). This would, in turn, channel the inflow of Atlantic water almost entirely through the Fram Strait, probably with higher flow velocities. It is however striking that the major change in ice sheet expansion in the Barents Sea at around 1 Ma is not reflected in the drift bodies along the western flank of the Yermak Plateau, while the onset of the northern hemisphere glaciation at around 2.7 Ma apparently led to a major change in suspension load and likely also changes in the current patterns.

7 Conclusion

The compilation of seismic profiles from the Fram Strait revealed large-scale drift sediments along the western Yermak Plateau flank. North of 80.5°N, a large field of sediment waves were encountered that separate a western, deeper from an eastern, shallower drift body. A seismostratigraphic boundary is clearly visible within the drift bodies and even more distinct within the sediment waves. Correlations with ODP Leg 151 Hole 911 reveal that this coincides with the boundary between lithostratigraphic units IA and IB, corresponding to seismic units YP-3 and YP-2. This boundary was dated to 2.7 Ma (Hull et al., 1996), which corresponds to the major ice-sheet expansion of the Greenland, Scandinavian and North American ice sheets. Sediment waves exhibit a shift to much higher migration angles of the wave crests at 2.7 Ma. This implies significantly increased sedimentation rates, pointing at a much higher suspension load of the West Spitsbergen Current and of the Yermak Branch. The Barents shelf which was subaerially exposed until ~1 Ma (Butt et al., 2002), which makes it a likely source area, later on replaced by Svalbard.

8 Acknowledgements

We thank all expedition and crewmembers of *RV Polarstern* ARK-XIII/3, ARK-XVIII/2 and ARK-XX/3 for their excellent work onboard. Special thanks go to the watch keepers of the bathymetry, seismic and sediment echosounder systems. We thank Pia Pulm who carried out extensive work on the profiles on the western flank of the Yermak Plateau for her diploma thesis, and Dr. Daniela Berger who worked on the profiles from the central Fram Strait for her PhD thesis. Maps were generated using the Generic Mapping Tools software (Wessel and Smith, 1991) and the IBCAO v.3 chart (Jakobsson et al., 2012).

9 References

Berger, D., 2009. Sedimentation history along the East Greenland margin, Alfred Wegener Institute Bremerhaven. University of Bremen, PhD thesis, Bremen, p. 134.

Berger, D., Jokat, W., 2008. A seismic study along the East Greenland margin from 72°N to 77°N. Geophysical Journal International 174, 733-748.

Berger, D., Jokat, W., 2009. Sediment deposition in the northern basins of the North Atlantic and characteristic variations in shelf sedimentation along the East Greenland margin. Marine and Petroleum Geology 26, 1321-1337.

Beszczynska-Möller, A., Fahrbach, E., Schauer, U., Hansen, E., 2012. Variability in Atlantic water temperature and transport at the entrance to the Arctic Ocean, 1997-2010. ICES Journal of Marine Sciences 69, 852-863.

Bourke, R.H., Weigel, A.M., Paquette, R.G., 1988. The Westward Turning Branch of the West Spitsbergen Current. Journal of Geophysical Research 93, 14065-14077.

Brigham-Grette, J., Melles, M., Minyuk, P.S., Andreev, A.A., Tarasov, P., DeConto, R.M., König, S., Nowaczyk, N.R., Wennrich, V., Rosén, P., Haltia-Hovi, E., Cook, T.L., Gebhardt, A.C., Meyer-Jacob, C., Snyder, J., Herzschuh, U., 2013. Pliocene warmth, extreme polar amplification, and stepped Pleistocene cooling recorded in NE Russia. Science.

Butt, F.A., Drange, H., Elverhøi., A., Otterå, O.H., Solheim, A., 2002. Modelling Late Cenozoic isostatic elevation changes in the Barents Sea and their implications for oceanic and climatic regimes: preliminary results. Quaternary Science Reviews 21, 1643-1660.

Dowdeswell, J.A., Jakobsson, M., Hogan, K.A., O'Regan, M., Backman, J., Evans, J., Hell, B., Löwemark, L., Marcussen, C., Noormets, R., Ó Cofaigh, C., Sellén, E., Sölvsten, M., 2010. High-resolution geophysical observations of the Yermak Plateau and northern Svalbard margin: implications for ice-sheet grounding and deep-keeled icebergs. Quaternary Science Reviews 29, 3518-3531.

Ehlers, B.-M., Jokat, W., 2013. Paleo-bathymetry of the northern North Atlantic and consequences for the opening of the Fram Strait. Marine Geophysical Research, 1-19.

Eiken, O., Hinz, K., 1993. Contourites in the Fram Strait. Sedimentary Geology 82, 15-32.

Fahrbach, E., Meincke, J., Østerhus, S., Rohardt, G., Schauer, U., Tverberg, V., Verduin, J., 2001. Direct measurements of volume transports through Fram Strait. Polar Research 20, 217-224.

Faugères, J.-C., Mulder, T., 2011. Contour Currents and Contourite Drifts, In: Huneke, H., Mulder, T. (Eds.), Developments in Sedimentology. Elsevier, pp. 149-214.

Faugères, J.-C., Stow, D.A.V., 2008. Contourite drifts: Nature, Evolution and Controls In: Rebesco, M., Camerlenghi, A. (Eds.), Contourites. Developments in Sedimentology, pp. 259-288.

Faugères, J.-C., Stow, D.A.V., Imbert, P., Viana, A., 1999. Seismic features diagnostic of contourite drifts. Marine Geology 162, 1-38.

Fieg, K., Gerdes, R., Fahrbach, E., Beszczynska-Möller, A., Schauer, U., 2010. Simulation of oceanic volume transports through Fram Strait 1995-2005. Ocean Dynamics 60, 491-502.

Flesche Kleiven, H., Jansen, E., Fronval, T., Smith, T.M., 2002. Intensification of Northern Hemisphere glaciations in the circum Atlantic region (3.5-2.4 Ma) - ice-rafted detritus evidence. Palaeogeography, Palaeoclimatology, Palaeoecology 184, 213-223.

519 Gebhardt, A.C., Jokat, W., Niessen, F., Matthiessen, J., Geissler, W.H., Schenke, H.-W., 2011.
520 Ice sheet grounding and iceberg plow marks on the northern and central Yermak
521 Plateau revealed by geophysical data. Quaternary Science Reviews 30, 1726-1738.
522 Geissler, W.H., Jokat, W., 2004. A geophysical study of the northern Svalbard continental
523 margin. Geophysical Journal International 158, 50-66.
524 Geissler, W.H., Jokat, W., Brekke, H., 2011. The Yermak Plateau in the Arctic Ocean in the
525 light of reflection seismic data – implication for its tectonic and sedimentary evolution.
526 Geophysical Journal International 187, 1334-1362.
527 Gradstein, F.M., Ogg, J.G., Hilgen, F.J., 2012. On the geologic time scale. Newsletter on
528 Stratigraphy 45, 171-188.
529 Haley, B.A., Frank, M., Spielhagen, R.F., Eisenhauer, A., 2008. Influence of brine formation
530 on Arctic Ocean circulation over the past 15 million years. Nature Geoscience 1.
531 Haug, G.H., Ganopolski, A., Sigman, D.M., Rosell-Mele, A., Swann, G.E.A., Tiedemann, R.,
532 Jaccard, S.L., Bollmann, J., Maslin, M.A., Leng, M.J., Eglinton, G., 2005. North Pacific
533 seasonality and the glaciation of North America 2.7 million years ago. Nature 433, 821-
534 825.
535 Howe, J.A., Livermore, R.A., Maldonaldo, A., 1998. Mudwave activity and current-
536 controlled sedimentation in Powell Basin, northern Weddell Sea, Antarctica. Marine
537 Geology 149, 229-241.
538 Howe, J.A., Shimmield, T.M., Harland, R., 2008. Late Quaternary contourites and
539 glaciomarine sedimentation in the Fram Strait. Sedimentology 55, 179-200.
540 Hull, D., Ostermann, L.E., Thiede, J., 1996. Biostratigraphic synthesis of Leg 151, North
541 Atlantic-Arctic Gateway, In: Thiede, J., Myhre, A.M., Firth, J.V., Johannessen, O.M.,
542 Ruddiman, W.F. (Eds.), Proceedings of the Ocean Drilling Program, Scientific Results, pp.
543 627-644.
544 Jakobsson, M., Backman, J., Rudels, B., Nycander, J., Frank, M., Mayer, L.A., Jokat, W.,
545 Sangiorgi, F., O'Regan, M., Brinkhuis, H., King, J.W., Moran, K., 2007. The early Miocene
546 onset of a ventilated circulation regime in the Arctic Ocean. Nature 447, 986-990.
547 Jakobsson, M., Macnab, R., Mayer, L.A., Anderson, R., Edwards, M.H., Hatzky, J., Schenke,
548 H.W., Johnson, P.D., 2008. An improved bathymetric potrayal of the Arctic Ocean:
549 Implication for an ocean modeling and geological, geophysical and oceanographic
550 analyses. Geophysical Research Letters 35, L07602.
551 Jakobsson, M., Mayer, L.A., Coakley, B., Dowdeswell, J.A., Forbes, S., Fridman, B.,
552 Hodnesdal, H., Noormets, R., Pedersen, R., Rebesco, M., Schenke, H.-W., Zarayskaya A, Y.,
553 Accettella, D., Armstrong, A., Anderson, R.M., Bienhoff, P., Camerlenghi, A., Church, I.,
554 Edwards, M., Gardner, J.V., Hall, J.K., Hell, B., Hestvik, O.B., Kristoffersen, Y., Marcussen, C.,
555 Mohammad, R., Mosher, D., Nghiem, S.V., Pedrosa, M.T., Travaglini, P.G., Weatherall, P.,
556 2012.
557 The International Bathymetric Chart of the Arctic Ocean (IBCAO) Version 3.0.
558 Geophysical Research Letters.
559 Jakobsson, M., Nilsson, J., O'Regan, M., Backman, J., Löwemark, L., Dowdeswell, J.A.,
560 Mayer, L., Polyak, L., Colleoni, F., Anderson, L.G., Björk, G., Darby, D., Eriksson, B., Hanslik,
561 D., Hell, B., Marcussen, C., Sellén, E., Wallin, Å., 2010. An Arctic Ocean ice shelf during MIS
562 6 constrained by new geophysical and geological data. Quaternary Science Reviews 29,
563 3505-3517
564 Jokat, W., 2003. The Expedition ARKTIS XVIII/2 of RV "Polarstern" in 2002 -
565 Contributions of the Participants.
566 Jokat, W., Geissler, W.H., Voss, M., 2008. Basement structure of the north-western
567 Yermak Plateau. Geophysical Research Letters 35, L05309.

568 Knies, J., Matthiessen, J., Mackensen, A., Stein, R., Vogt, C., Frederichs, T., Nam, S.-I., 2007.
569 Effects of Arctic freshwater forcing on thermohaline circulation during the Pleistocene.
570 Geology 35, 1075-1078.
571 Knies, J., Matthiessen, J., Vogt, C., Laberg, J.S., Hjelstuen, B.O., Smelror, M., Larsen, E.,
572 Andreassen, K., Eidvin, T., Vorren, T.O., 2009. The Plio-Pleistocene glaciation of the
573 Barents Sea-Svalbard region: a new model based on revised chronostratigraphy.
574 Quaternary Science Reviews 28, 812-829.
575 Krause, G., 1998. The Expedition ARKTIS-XIII/3 of RV "Polarstern" in 1997.
576 Laberg, J.S., Andreassen, K., Knies, J., Vorren, T.O., Winsborrow, M., 2010. Late Pliocene-
577 Pleistocene development of the Barents Sea Ice Sheet. Geology 38, 107-110.
578 Läderach, C., Schlindwein, V., Schenke, H.-W., Jokat, W., 2011. Seismicity and active
579 tectonic processes in the ultra-slow spreading Lena Trough, Arctic Ocean. Geophysical
580 Journal International 184, 1354-1370.
581 Manley, T.O., Bourke, R.H., Hunkins, K.L., 1992. Near-surface circulation over the Yermak
582 plateau in northern Fram Strait. Journal of Marine Systems 3, 107-125.
583 Melles, M., Brigham-Grette, J., Minyuk, P.S., Nowaczyk, N.R., Wennrich, V., DeConto, R.M.,
584 Anderson, P.M., Andreev, A.A., Coletti, A., Cook, T.L., Haltia-Hovi, E., Kukkonen, M.,
585 Lozhkin, A.V., Rosén, P., Tarasov, P., Vogel, H., Wagner, B., 2012. 2.8 million years of
586 Arctic climate change from Lake El'gygytgyn, NE Russia. Science 337, 315-320.
587 Moran, K., Backman, J., Brinkhuis, H., Clemens, S.C., Cronin, T., Dickens, G.R., Eynaud, F.,
588 Gattacceca, J., Jakobsson, M., Jordan, R.W., Kaminski, M., King, J.W., Koc, N., Krylov, A.,
589 Martinez, N., Matthiessen, J., McInroy, D., Moore, T.C., Onodera, J., O'Regan, M., Pälike, H.,
590 Rea, B., Rio, D., Sakamoto, T., Smith, D.C., Stein, R., St John, K., Suto, I., Suzuki, N.,
591 Takahashi, K., Watanabe, M., Yamamoto, M., Farrell, J., Frank, M., Kubik, P., Jokat, W.,
592 Kristoffersen, Y., 2006. The Cenozoic palaeoenvironment of the Arctic Ocean. Nature
593 441, 601-605.
594 Mudelsee, M., Raymo, M.E., 2005. Slow dynamics of the Northern Hemisphere glaciation.
595 Paleoceanography 20, PA4022.
596 Myhre, A.M., Thiede, J., Firth, J.V., Ahagon, N., Black, K.S., Bloemendal, J., Brass, G.W.,
597 Bristow, J.F., Chow, N., Cremer, M., Davis, L., Flower, B., Fronval, T., Hood, J., Hull, D., Koç,
598 N., Larsen, B., Lyle, M., McManus, J., O'Connel, S., Ostermann, L.E., Rack, F.R., Sato, T.,
599 Scherer, R., Spiegler, D., Stein, R., Tadross, M., Wells, S., Williamson, D., Witte, B., Wolf-
600 Welling, T., 1995. Proceedings of the Ocean Drilling Program, Initial Reports, Leg 151.
601 College Station, Texas.
602 O'Regan, M., Jakobsson, M., Kirchner, N., 2010. Glacial geological implications of
603 overconsolidated sediments on the Lomonosov Ridge and Yermak Plateau. Quaternary
604 Science Reviews 29, 3532-3544.
605 Ó Cofaigh, C., Dowdeswell, J.A., Evans, J., Kenyon, N.H., Taylor, J., Mienert, J., Wilken, M.,
606 2004. Timing and significance of glacially influenced mass-wasting in the submarine
607 channels of the Greenland Basin. Marine Geology 207, 39-54.
608 Pulm, P., 2010. Sedimentation processes in the northern Fram Strait since early Miocene,
609 Fakultät für Mathematik, Informatik und Naturwissenschaften. University of Hamburg,
610 Diploma thesis, Hamburg, p. 218.
611 Quadfasel, D., Gascard, J.-C., Koltermann, K.-P., 1987. Large-scale oceanography in Fram
612 Strait during the 1984 Marginal Ice Zone Experiment. Journal of Geophysical Research,
613 6719-6728.
614 Ravelo, A.C., 2010. Warmth and glaciation. Nature Geoscience 3, 672-674.
615 Rudels, B., Björk, G., Nilsson, J., Winsor, P., Iréne, L., Nohr, C., 2005. The interaction
616 between waters from the Arctic Ocean and the Nordic Seas north of Fram Strait and

along the East Greenland Current: results from the Arctic Ocean-02 Oden expedition. Journal of Marine Systems 55, 1-30.
Rudels, B., Fahrbach, E., Meincke, J., Budeus, G., Eriksson, P., 2002. The East Greenland Current and its contribution to the Denmark Strait overflow. ICES Journal of Marine Science: Journal du Conseil 59, 1133-1154.
Rudels, B., Korhonen, M., Budéus, G., Beszczynska-Möller, A., Schauer, U., Nummelin, A., Quadfasel, D., Valdimarsson, H., 2012. The East Greenland Current and its impacts on the Nordic Seas: observed trends in the past decade. ICES Journal of Marine Sciences 69, 1-11.
Rutgers van der Loeff, M.M., Meyer, R., Rudels, B., Rachor, E., 2002. Resuspension and particle transport in the benthic nepheloid layer in and near Fram Strait in relation to faunal abundances and ^{234}Th depletion. Deep-Sea Research I 49, 1941-1958.
Sarkar, S., Berndt, C., Chabert, A., Masson, D.G., Minshull, T.A., Westbrook, G.K., 2011. Switching of a paleo-ice stream in northwest Svalbard. Quaternary Science Reviews 30, 1710-1725.
Sato, T., Kameo, K., 1996. Pliocene to Quaternary calcareous nannofossil biostratigraphy of the Arctic Ocean, with reference to late Pliocene glaciation, In: Thiede, J., Myhre, A.M., Firth, J.V., Johnson, G.L., Ruddiman, W.F. (Eds.), Proceedings Ocean Drilling Program. Scientific results, pp. 39-59.
Schauer, U., Fahrbach, E., Osterhus, S., Rohardt, G., 2004. Arctic warming through the Fram Strait: Oceanic heat transport from 3 years of measurements. Journal of Geophysical Research 109.
Schlichtholz, P., Houssais, M.-N., 1999. An inverse modeling study in Fram Strait. Part I: dynamics and circulation. Deep-Sea Research II 46, 1083-1135.
Stein, R., 2005. Scientific Cruise Report of the Arctic Expedition ARK-XX/3 of RV "Polarstern" in 2004: Fram Strait, Yermak Plateau and East Greenland Continental Margin.
Tripati, A.K., Eagle, R.A., Morton, A., Dowdeswell, J.A., Atkinson, K.L., Bahé, Y., Dawber, C.F., Khadun, E., Shaw, R.M.H., Shorttle, O., Thanabalasundaram, L., 2008. Evidence for glaciation in the Northern Hemisphere back to 44 Ma from ice-rafted debris in the Greenland Sea. Earth and Planetary Science Letters 265, 112-122.
Vogt, P.R., Crane, K., Sundvor, E., 1994. Deep Pleistocene iceberg plowmarks on the Yermak Plateau: Sidescan and 3.5 kHz evidence for thick calving ice fronts and a possible marine ice sheet in the Arctic Ocean. Geology 22, 403-406.
Wessel, P., Smith, W.H.F., 1991. Free software helps map and display data, EOS Trans. AGU, 72, 441, 1991. Eos Transactions AGU 72, 441.
Winkler, A., Wolf-Welling, T.C.W., Stattegger, K., Thiede, J., 2002. Clay mineral sedimentation in high northern latitude deep-sea basins since the Middle Miocene (ODP Leg 151, NAAG). International Journal of Earth Sciences 91, 133-148.
Wynn, R.B., Masson, D.G., 2008. Sediment waves and bedforms, In: Rebesco, M., Camerlenghi, A. (Eds.), Contourites, pp. 289-300.

Figure Captions

Fig. 1: Geographical overview of the Fram Strait and its surroundings. Blue and red arrows mark the present-day predominant surface water flows in this area (Manley et al., 1992). Spacing of bathymetry contour lines is 500 m down to 2000 m water depth and 1000 m at >2000 m water depth. Map was created from the IBCAO dataset (Jakobsson et al., 2008) using GMT software tools (Wessel and Smith, 1991). Geographical names: SvB: Sverdrup Bank; Currents: EGC: East Greenland Current, RAC: Return Atlantic Current, SpB: Spitsbergen Branch, WSC: Western Spitsbergen Current, YB: Yermak Branch. The yellow stars mark the positions of ODP Leg 151 Sites 909 to 912. Tracklines of the seismic profiles used in this study are shown in white; those mentioned in the text and/or shown in other figures are labeled and shown in yellow. The red part of profile AWI-20040080 is shown in figure 7a, and the red rectangle marks the position of the bathymetry detail in figure 7b. The dashed pink line at 79° marks the approximate position of the oceanographic transect in figure 9.

Fig. 2: Compilation of age information used for this study. Timescale after Gradstein et al. (2012), ODP Leg 151 age information from Winkler et al. (2002) and Hull et al. (1996), additional age information on site 909 (i.e., subdivision of Unit I into IA* and IB*) from Knies et al. (2009), and seismostratigraphic information from Geissler and Jokat (2004) and Geissler et al. (2011).

Fig. 3: Upper panel: Interpreted line drawing of seismic profile AWI-20040040 showing the drift bodies “A” and “B” and the field of sediment waves in between. Grey shading indicates the acoustic basement along the profile. Seismostratigraphic unit YP-3 is shown in yellow, YP-2 in orange, and oldest unit YP-1 in green. Lower panel: Unmigrated section of profile AWI-20040040. Trackline of entire profile AWI-20040040 is shown in Fig. 1. Seismostratigraphic units (YP-1 to YP-3) are named after the nomenclature by Geissler et al. (2011), lithostratigraphic unit numbering (IA to IC) according to Site 910 (Hull et al., 1996).

Fig. 4: Upper panel: Interpreted line drawing of seismic profile AWI-20040150 showing the drift bodies “A” and “B” and the field of sediment waves in between. Grey shading indicates the acoustic basement along the profile. Seismostratigraphic unit YP-3 is shown in yellow, YP-2 in orange, and oldest unit YP-1 in green. Lower panel: Unmigrated section of profile AWI-20040150. Trackline of entire profile AWI-20040150 is shown in Fig. 1.

Fig. 5: Upper panel: Interpreted line drawing of seismic profile AWI-20040160 showing the drift bodies “A” and “B” and the field of sediment waves in between. Grey shading indicates the acoustic basement along the profile. Seismostratigraphic unit YP-3 is shown in yellow, YP-2 in orange, and oldest unit YP-1 in green. Lower panel: Unmigrated section of profile AWI-20040160. Trackline of entire profile AWI-20040160 is shown in Fig. 1. The orange rectangle in the lower panel marks the position of the detailed view shown in Fig. 6.

Fig. 6: Detailed view of the sediment waves observed in profile AWI-20040160. Upper panel: Interpreted line drawing. Lower panel: Unmigrated section.

Fig. 7: Upper panel: Interpreted line drawing of seismic profile AWI-97253 showing a channel-levée complex. Grey shading indicates the acoustic basement along the profile. Seismostratigraphic units IA* is shown in yellow, IB* in orange, II in turquoise, IIIA in blue and IIIB in lilac. A huge mass movement deposit is marked by dots. Lower panel: Unmigrated section of profile AWI-97253. Trackline of entire profile AWI-97253 is shown in Fig. 1.

Fig. 8: Position of drift body A (in lilac), drift body B (in green), upper sediment wave package (in orange) and lower sediment wave package (hatched). The red ovals mark the positions of the levées identified on profile AWI-97253. ODP Leg 151 Sites 909 to 912 are marked with yellow stars.

Fig. 9: a. Detail of the sediment waves in profile AWI-20040080. **b**. Bathymetry data of parts of the sediment wave field. Crest orientation is marked in pink. Trackline of a. and position of b. are shown in figure 1.

Fig. 10: Oceanographic profile at 79°N (modified after Fieg et al., 2010; and after Pulm, 2010).

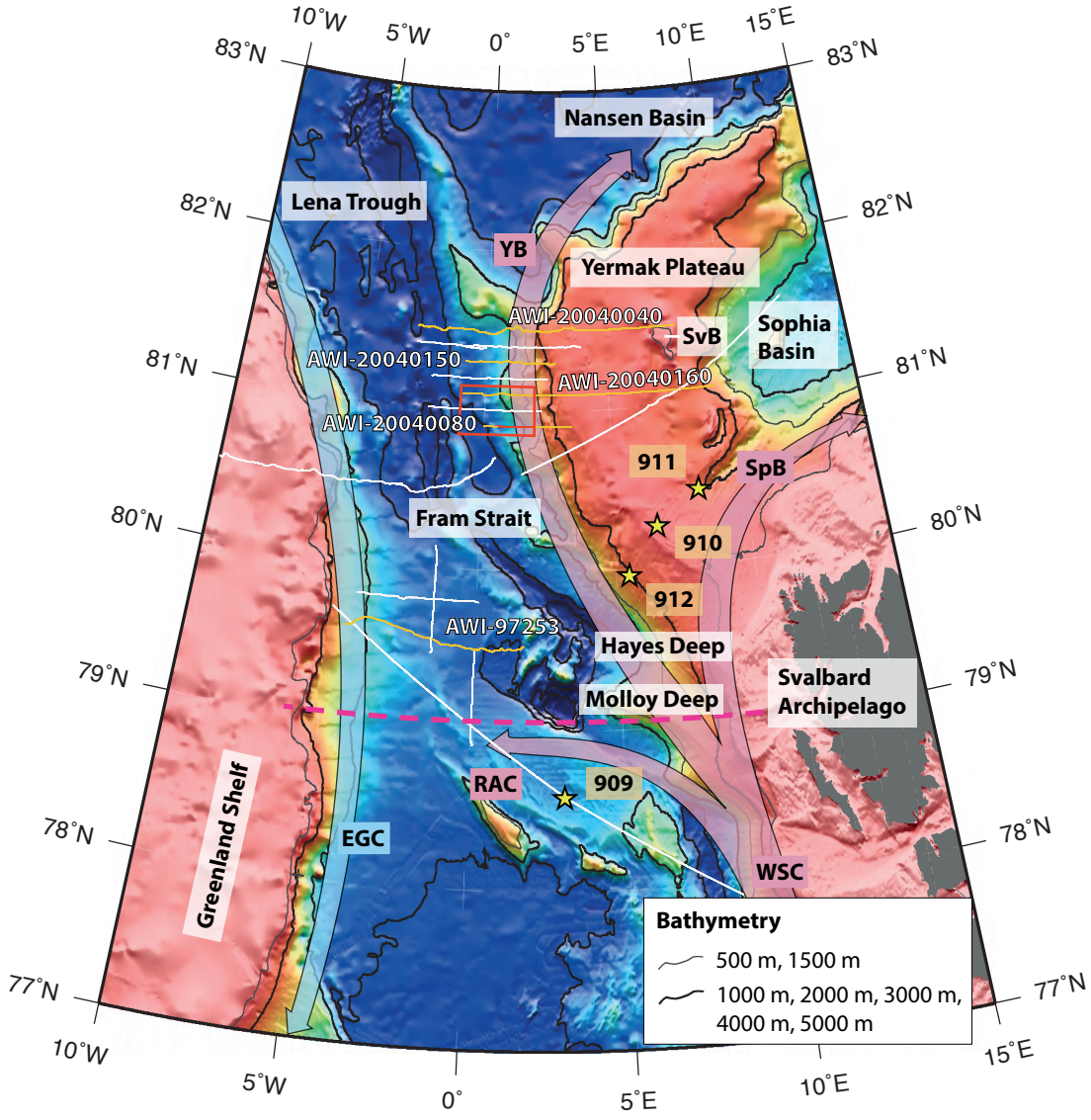
10°W
5°W
0°
5°E
10°E
15°E
83°N
82°N
81°N
80°N
79°N
78°N
77°N
Nansen Basin
Lena Trough
YB
Yermak Plateau
AWI-20040040
SvB
Sophia Basin
AWI-20040150
AWI-20040160
AWI-20040080
911
SpB
Fram Strait
910
912
AWI-97253
Hayes Deep
Molloy Deep
Svalbard Archipelago
RAC
909
Greenland Shelf
EGC
WSC
Bathymetry
500 m, 1500 m
1000 m, 2000 m, 3000 m, 4000 m, 5000 m

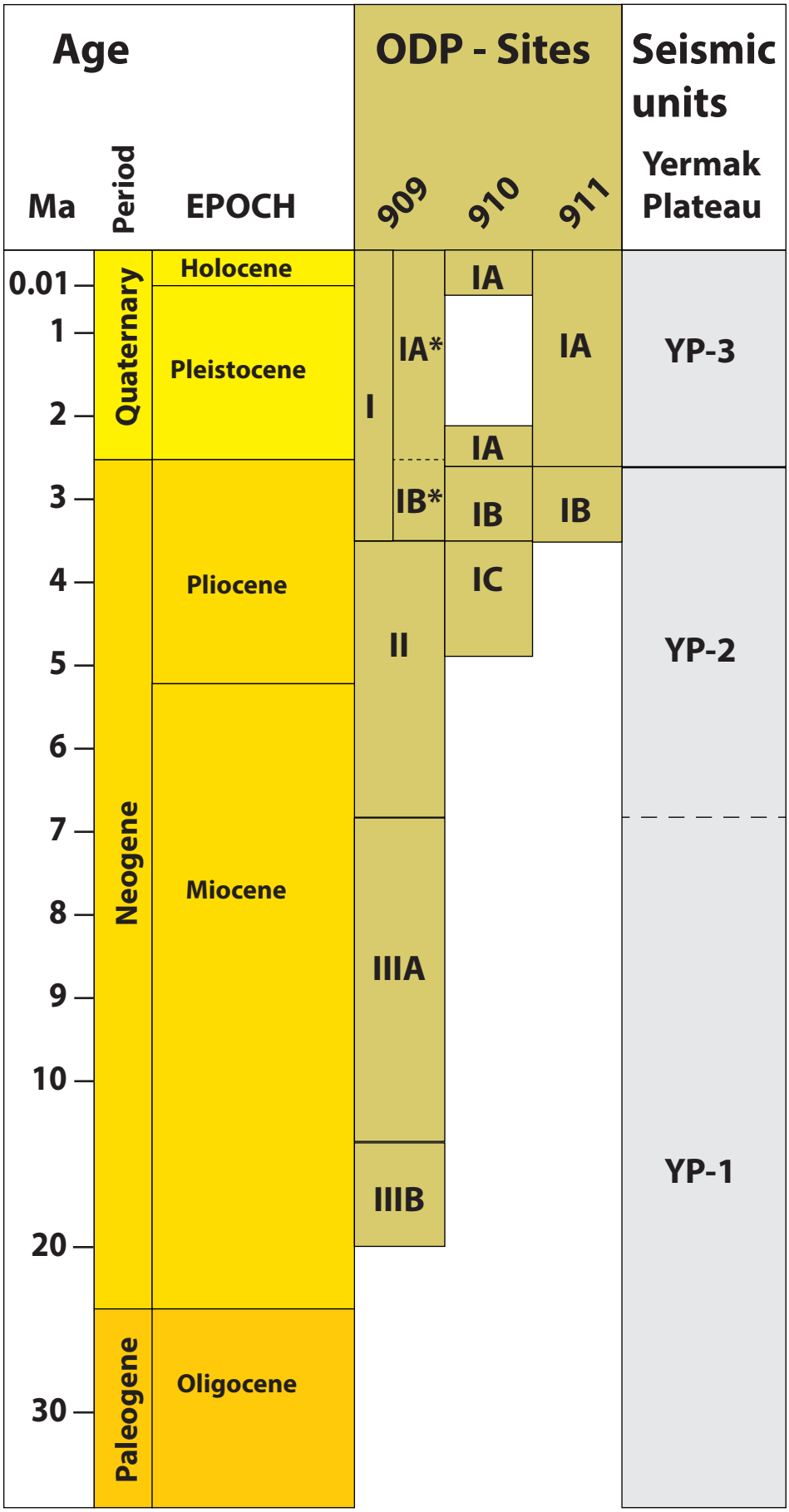
Age
Ma
Period
EPOCH
ODP - Sites
909
910
911
Seismic units
Yermak Plateau
0.01
1
2
3
4
5
6
7
8
9
10
20
30
Quaternary
Neogene
Paleogene
Holocene
Pleistocene
Pliocene
Miocene
Oligocene
I
IA*
IB*
II
IIIA
IIIB
IA
IA
IB
IA
IA
IB
IC
YP-3
YP-2
YP-1

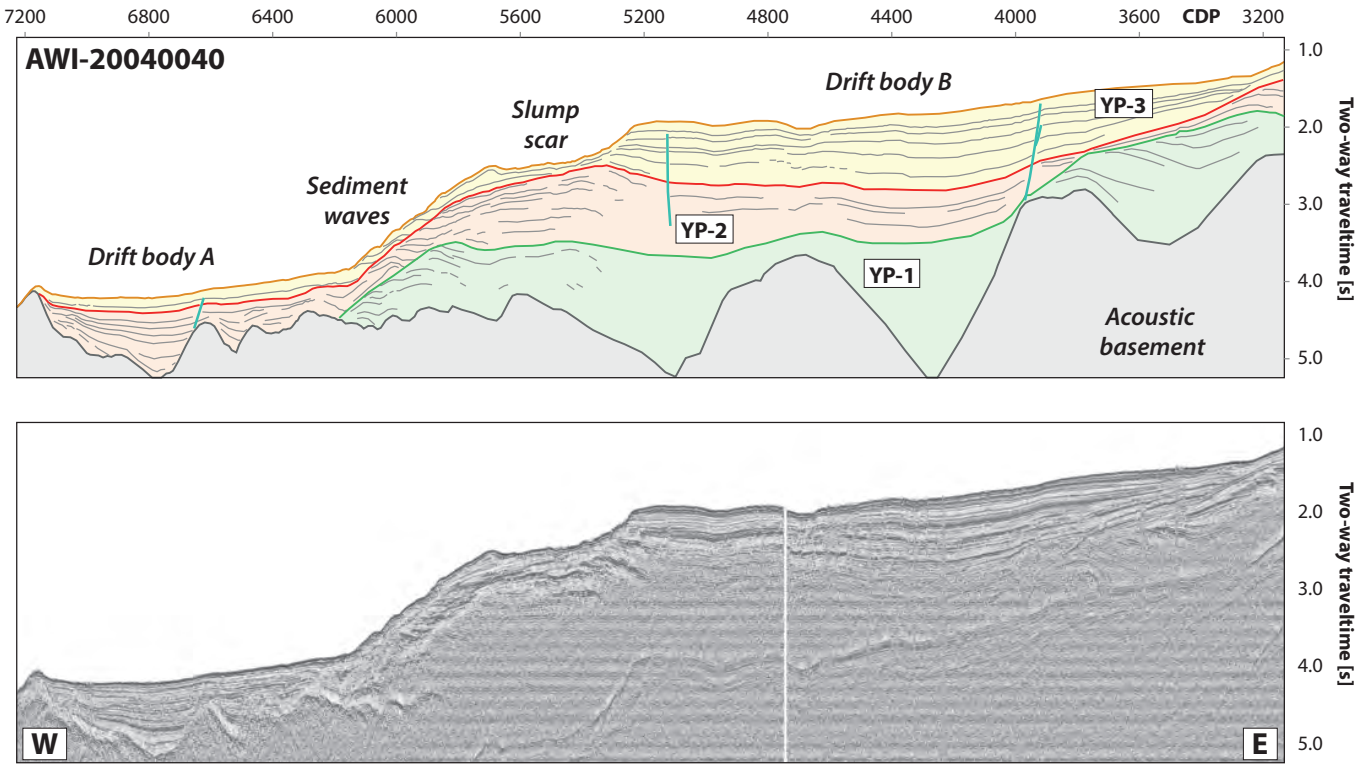
7200
6800
6400
6000
5600
5200
4800
4400
4000
3600
CDP
3200
AWI-20040040
Drift body B
Slump scar
Sediment waves
Drift body A
YP-3
YP-2
YP-1
Acoustic basement
1.0
2.0
3.0
4.0
5.0
Two-way traveltime [s]
W
E

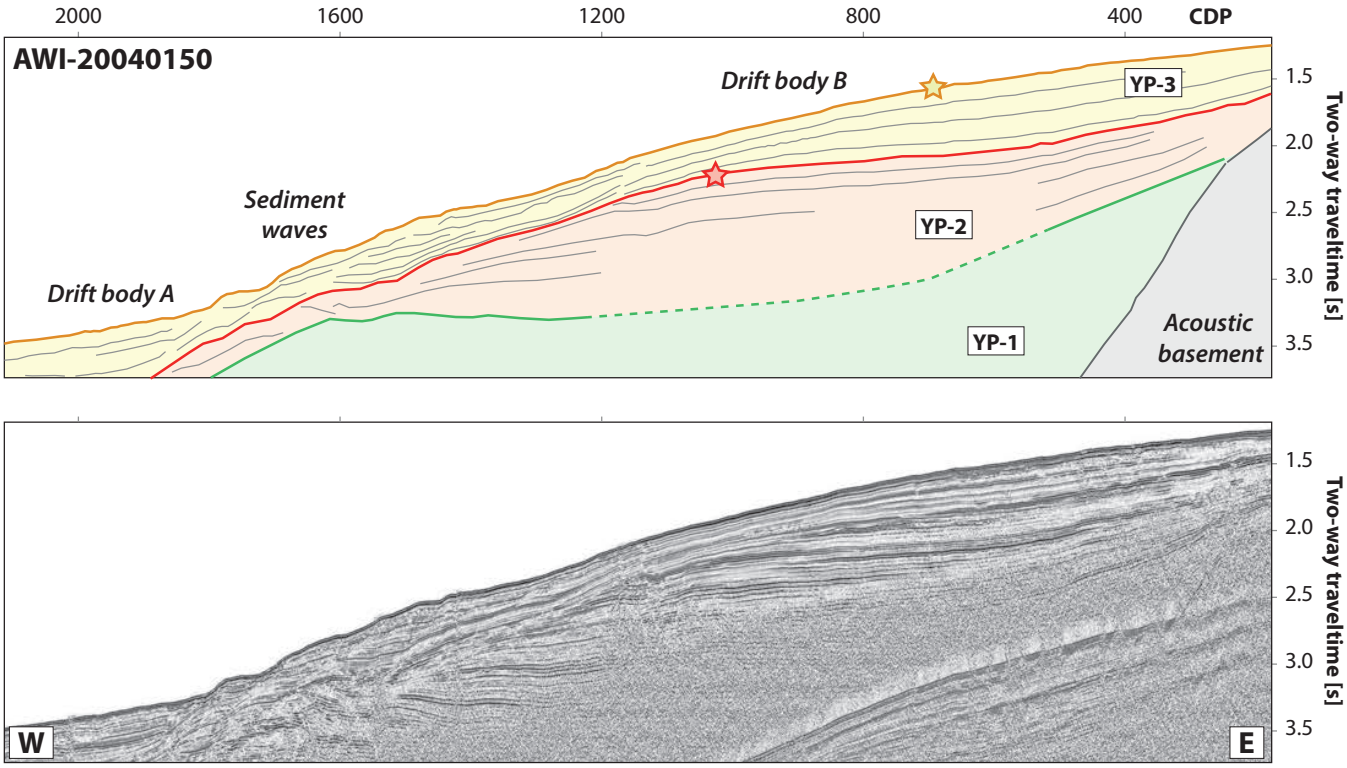
2000
1600
1200
800
400
CDP
AWI-20040150
Drift body B
YP-3
Sediment waves
YP-2
Drift body A
YP-1
Acoustic basement
1.5
2.0
2.5
3.0
3.5
Two-way traveltime [s]
W
E

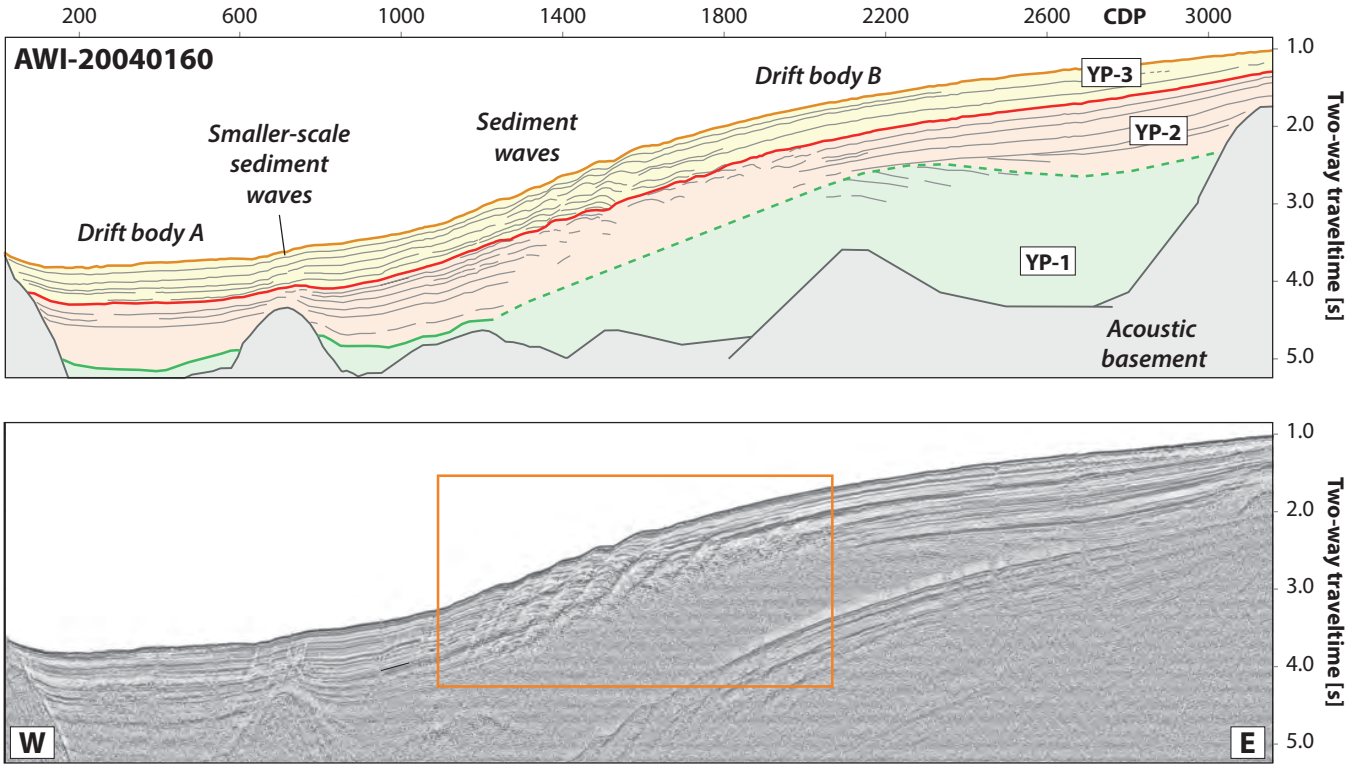
200
600
1000
1400
1800
2200
2600
CDP
3000
AWI-20040160
Drift body B
YP-3
YP-2
Smaller-scale sediment waves
Sediment waves
Drift body A
YP-1
Acoustic basement
1.0
2.0
3.0
4.0
5.0
Two-way traveltime [s]
W
E

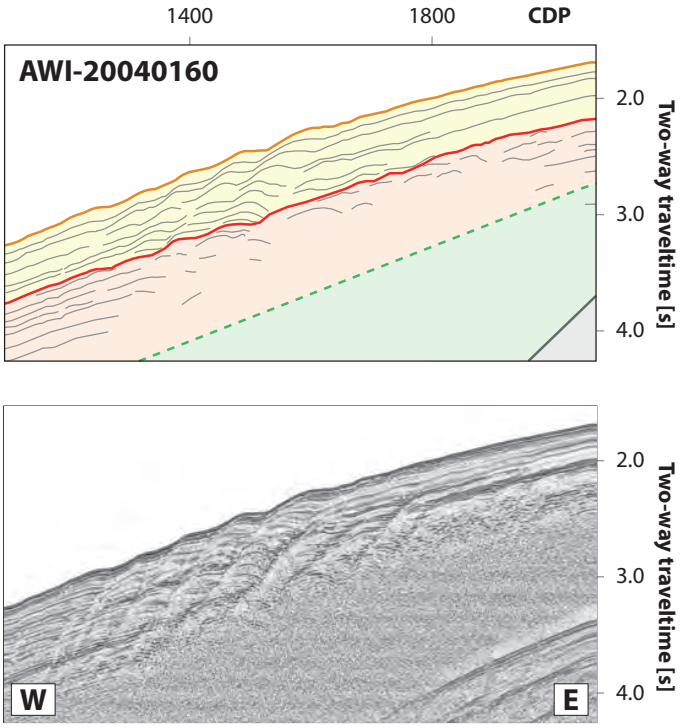
1400
1800
CDP
AWI-20040160
2.0
3.0
4.0
Two-way traveltime [s]

W
E
2.0
3.0
4.0
Two-way traveltime [s]

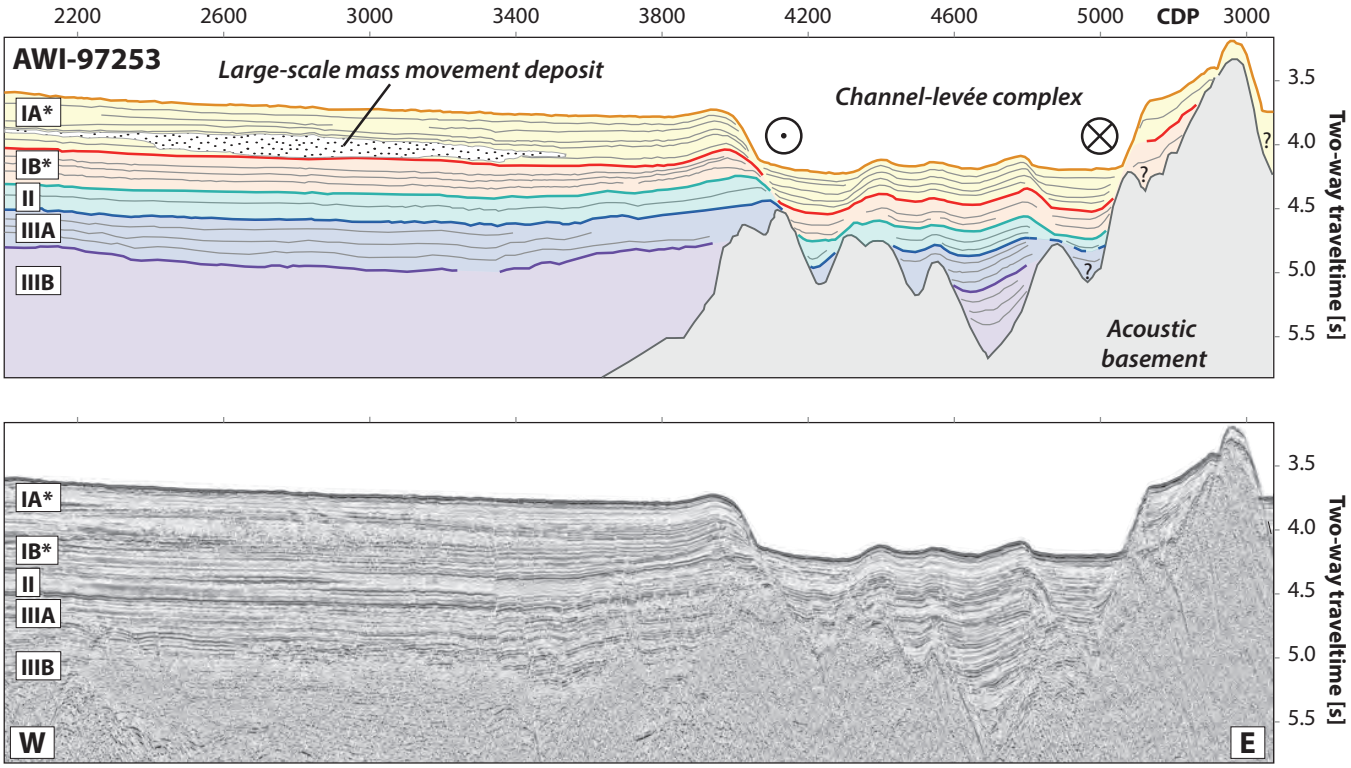
2200
2600
3000
3400
3800
4200
4600
5000
CDP
3000
AWI-97253
Large-scale mass movement deposit
Channel-levée complex
IA*
IB*
II
IIIA
IIIB
Acoustic basement
3.5
4.0
4.5
5.0
5.5
Two-way traveltime [s]
W
E

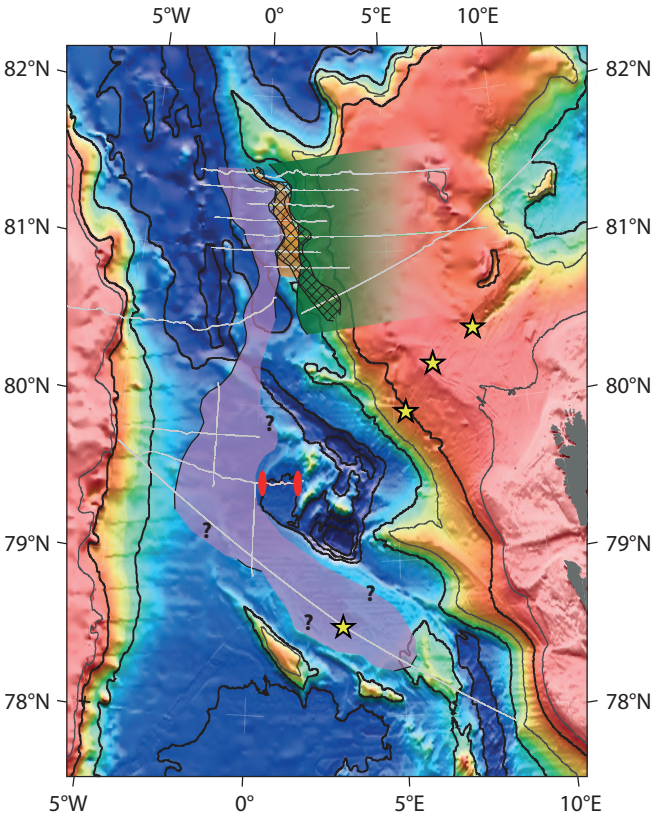
5°W
0°
5°E
10°E
82°N
81°N
80°N
79°N
78°N
?
?
?

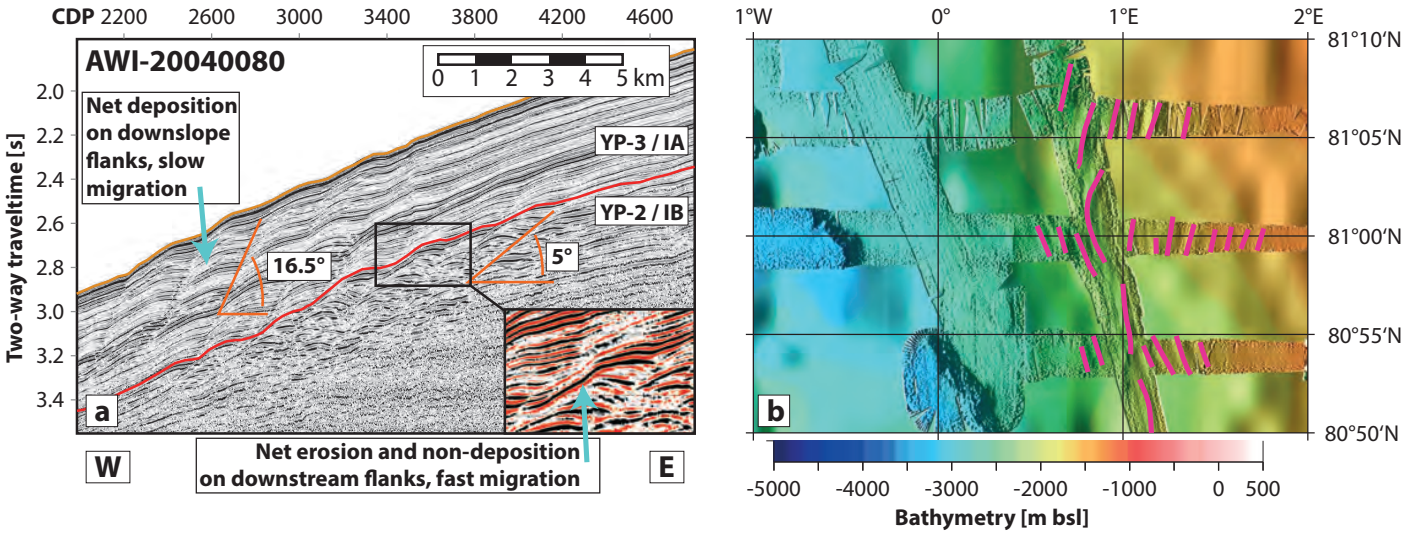
CDP 2200
2600
3000
3400
3800
4200
4600
AWI-20040080
0 1 2 3 4 5 km
Two-way traveltime [s]
2.0
2.2
2.4
2.6
2.8
3.0
3.2
3.4
Net deposition on downslope flanks, slow migration
YP-3 / IA
YP-2 / IB
16.5°
5°
a
W
Net erosion and non-deposition on downstream flanks, fast migration
E
1°W
0°
1°E
2°E
81°10'N
81°05'N
81°00'N
80°55'N
80°50'N
b
-5000
-4000
-3000
-2000
-1000
0
500
Bathymetry [m bsl]

Current velocities through the Fram Strait at 79°N

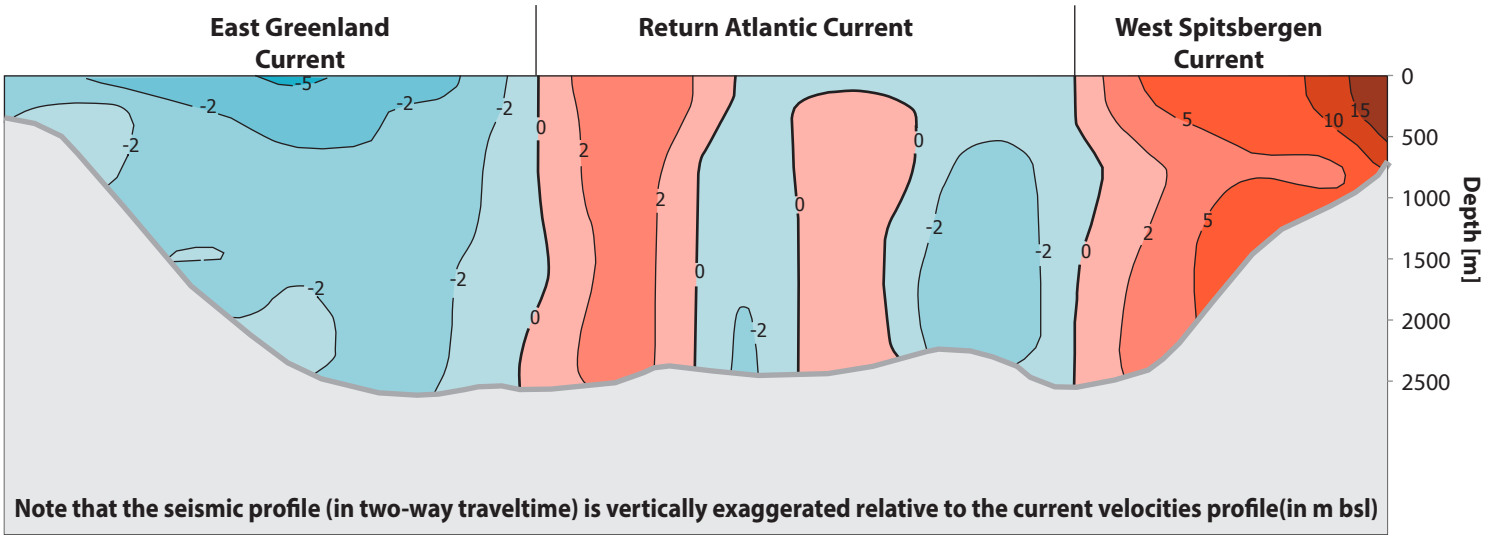

Note that the seismic profile (in two-way traveltime) is vertically exaggerated relative to the current velocities profile(in m bsl)

Current velocities towards north

- > 15 cm/s
- 10 - 15 cm/s
- 5 - 10 cm/s
- 2 - 5 cm/s
- 0 - 2 cm/s

Currents towards south

- 0 - -2 cm/s
- -2 - -5 cm/s
- -5 - -10 cm/s